Chapter 42
Shallow Gas and the Development of a Weak Layer in Submarine Spreading, Hikurangi Margin (New Zealand)

Aaron Micallef, Joshu J. Mountjoy, Sebastian Krastel, Gareth Crutchley, and Stephanie Koch

Abstract Submarine spreading is a type of mass movement that involves the extension and fracturing of a thin surficial layer of sediment into coherent blocks and their finite displacement on a gently sloping slip surface. Its characteristic seafloor signature is a repetitive pattern of parallel ridges and troughs oriented perpendicular to the direction of mass movement. We map ~30 km^2 of submarine spreads on the upper slope of the Hikurangi margin, east of Poverty Bay, North Island, New Zealand, using multibeam echosounder and 2D multichannel seismic data. These data show that spreading occurs in thin, gently-dipping, parallel-bedded clay, silt and sandy sedimentary units deposited as lowstand clinoforms. More importantly, high-amplitude and reverse polarity seismic reflectors, which we interpret as evidence of shallow gas accumulations, occur extensively in the fine sediments of the upper continental slope, but are either significantly weaker or entirely absent where the spreads are located. We use this evidence to propose that shallow gas, through the generation of pore pressure, has played a key role in establishing the failure surface above which submarine spreading occurred. Additional dynamic changes in pore pressure could have been triggered by a drop in sea level during the Last Glacial Maximum and seismic loading.

A. Micallef (✉)
University of Malta, Msida, Malta
e-mail: aaron.micallef@um.edu.mt; micallefaaron@gmail.com

J.J. Mountjoy
National Institute of Water and Atmospheric Research (NIWA), Wellington, New Zealand

S. Krastel
Christian-Albrechts-Universität zu Kiel, Kiel, Germany

G. Crutchley
GNS Science, Lower Hutt, New Zealand

S. Koch
GEOMAR, Kiel, Germany

G. Lamarche et al. (eds.), *Submarine Mass Movements and their Consequences*,
Advances in Natural and Technological Hazards Research 41,
DOI 10.1007/978-3-319-20979-1_42

42.1 Introduction

Spreading entails the finite and downslope surficial displacement of rock/sediment on gently sloping ground, and the fracturing of the displaced mass into coherent blocks (Varnes 1978). Displacement mostly occurs along a shear zone (Rohn et al. 2004), and the deformation may involve subsidence, translation, rotation and disintegration of the upper coherent units (Dikau et al. 1996; Varnes 1978). The ground deformation associated with spreading comprises the extensional fissuring of the surface units in the form of alternating ridges and troughs (Dikau et al. 1996). The literature on spreading is not as extensive and exhaustive as for other types of mass movement, and little is known about the mechanics of the failure process. Deformation in a spread is known to be driven by a combination of transient and static shear stresses, attributed to a loss of shear strength of the underlying sediment, which allows the overlying material to slide downslope as intact blocks. The geological conditions conducive to spreading are usually those where consolidated rocks or sediments overlie a ductile substratum (Dikau et al. 1996; Rohn et al. 2004). In terrestrial environments, spreading is inextricably linked to the build up of pore pressure and associated liquefaction, which may occur in shallow underlying deposits either during an earthquake or due to changes in the height of the water table (Kanibir et al. 2006).

In submarine settings, numerical and mechanical models have indicated that, similarly to terrestrial environments, an increase in pore pressure may be a key preconditioning factor and trigger of spreading (Kvalstad et al. 2005; Micallef et al. 2007). In this paper we address the hypothesis that, by influencing pore pressure in sub-seafloor sediment, shallow gas can promote the development of a weak layer above which submarine spreading can occur. We do this by analysing geophysical data acquired from offshore the east coast of North Island, New Zealand (Fig. 42.1).

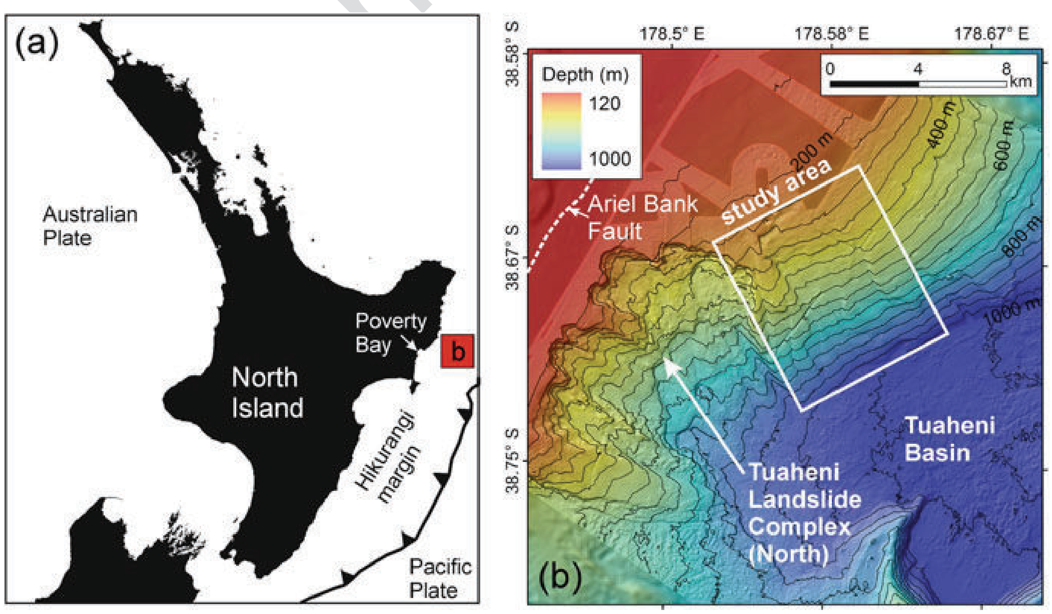

Fig. 42.1 (**a**) Location map. (**b**) Bathymetric map of the continental slope offshore Poverty Bay, showing location of study area. Isobaths at 50 m intervals

In comparison to terrestrial spreading, submarine spreading has received very little attention. First reported from offshore California (Field et al. 1982), most of what we know about submarine spreading comes from studies of the Norwegian passive continental margin (Baeten et al. 2013; Gauer et al. 2005; Kvalstad et al. 2005; Micallef et al. 2007, 2009). Nevertheless, the characteristic submarine spreading morphology, in the form of a recurring pattern of ridges and troughs, can be observed in numerous submarine landslides around the world (Lastras et al. 2003, 2006; Micallef et al. 2013; Piper et al. 1999; Vanneste et al. 2006). This means that submarine spreading is a widespread type of mass movement that has played an important role in the development of submarine landslides in different settings, and which therefore merits more detailed investigation.

42.2 Study Area

Our study area is located on the upper slope of the Hikurangi margin, 45 km east of Poverty Bay, North Island, New Zealand (Fig. 42.1). The east coast of the North Island straddles the boundary between the Pacific and Australian tectonic plates. This margin is characterised by the westward subduction of the Pacific Plate beneath the North Island, at a rate of about 4.5–5.5 cm year^{-1} (Beavan et al. 2002). Across the continental shelf in the region of our study area, active eastward verging splay faults from the plate boundary mega-thrust are known to project to the seafloor (Mountjoy and Barnes 2011). On the mid- to upper-slope, however, there is a lack of active tectonic deformation, which results in a relatively simple facies geometry. The upper continental slope of the Hikurangi margin is underlain by Miocene to recent slope basin sequences with possible Cretaceous and Paleogene sedimentary rocks at depth (Barnes et al. 2002; Mountjoy and Barnes 2011). Overlying these sequences at the shelf break are lowstand clinoforms deposited during the Quaternary glacial cycles (Barnes et al. 2002; Pedley et al. 2010). These deposits are formed of gently dipping, parallel-bedded clay, silt and possibly sandy sedimentary units (Alexander et al. 2010). Modest size (0.01 km^3) to very large (3,000 km^3) submarine landslides have occurred on the Hikurangi margin (Barnes et al. 2010; Kukowski et al. 2010). Some of the best preserved examples of these occur on the upper continental slope directly off Poverty Bay and to the south-west of the study area (Fig. 42.1b). These include the ~30 km^3 Poverty Debris Avalanche, and the ~10 km^3 Tuaheni Landslide Complex (Mountjoy et al. 2009).

42.3 Data and Methods

Our study is based on two types of data. The first is a multibeam echosounder dataset covering 700 km^2 of seafloor (Fig. 42.1b). These data were acquired using a hull-mounted Kongsberg EM300 multibeam system during two cruises (TAN1114 in 2011 and TAN0810 in 2008). The bathymetry data were processed with CARIS Hydrographic Information Processing System (HIPS) by accounting for sound velocity variations, tides and basic quality control. A bathymetry grid with 25×25 m bin size was derived. The second dataset comprises high resolution 2D multichannel seismic reflection data acquired during the TAN1404 cruise in 2014 (Fig. 42.2). The acquisition system entailed a 0.7 l GI Gun and a 150 m long streamer with 96 channels. Processing included crooked line common midpoint (CMP) binning (CMP spacing of 1.5 m), frequency filtering (Butterworth filter with low-cut corner frequencies of 25 and 55 Hz), normal move-out correction, stacking and 2D Stolt migration. All cruises were carried out on board the *R/V Tangaroa*.

42.4 Results

42.4.1 Morphology

The continental slope within the study area has an average slope gradient of 5.5° towards SSE. The morphology is dominated by an elongated scar with a length of 8 km, width of 4 km, and 60 m depth (Fig. 42.2a). The downslope limit of the scar coincides with the regional base of the continental slope where it is contiguous with the Tuaheni sedimentary basin, at 975 m depth. Its headwall is located in the upper continental slope, at a depth of 250 m. Smaller scars, sharing a similar morphology and distal limit, are located 1 km to the north-east of the elongated scar. The seafloor morphology across the upper section of the scar predominantly consists of a subdued, repetitive pattern of ridges and troughs oriented parallel to the isobaths. In the downslope section of the scar, the morphology is smoother and intersected by lineations that are up to 3 km long, 5 m deep, and oriented perpendicular to the isobaths. These lineations and the western boundary of the scar are intersected by a 4.5 km long and 20 m high SW-NE oriented escarpment. Circular depressions that are up to 200 m wide and 30 m deep are located at the headwall of the scar.

42.4.2 Sub-seafloor Architecture

The seismic expression of the sub-seafloor in the study area comprises a sequence of continuous, parallel, gently-dipping seismic reflectors that is at least 150 m thick in places (assuming a seismic P wave velocity of 1600 m s^{-1} for depth conversion). Two reflectors within this sequence are characterised by high amplitude and reverse polarity, and are recorded at an average depth of 55 m below the seafloor (Fig. 42.2b). These high amplitude reflectors occur across the upper continental slope, but are either significantly weaker or entirely absent where the elongated scar with the ridge and trough morphology is present. Here, the upper part of the seismic sequence is generally characterised by a unit of irregular, chaotic, low amplitude

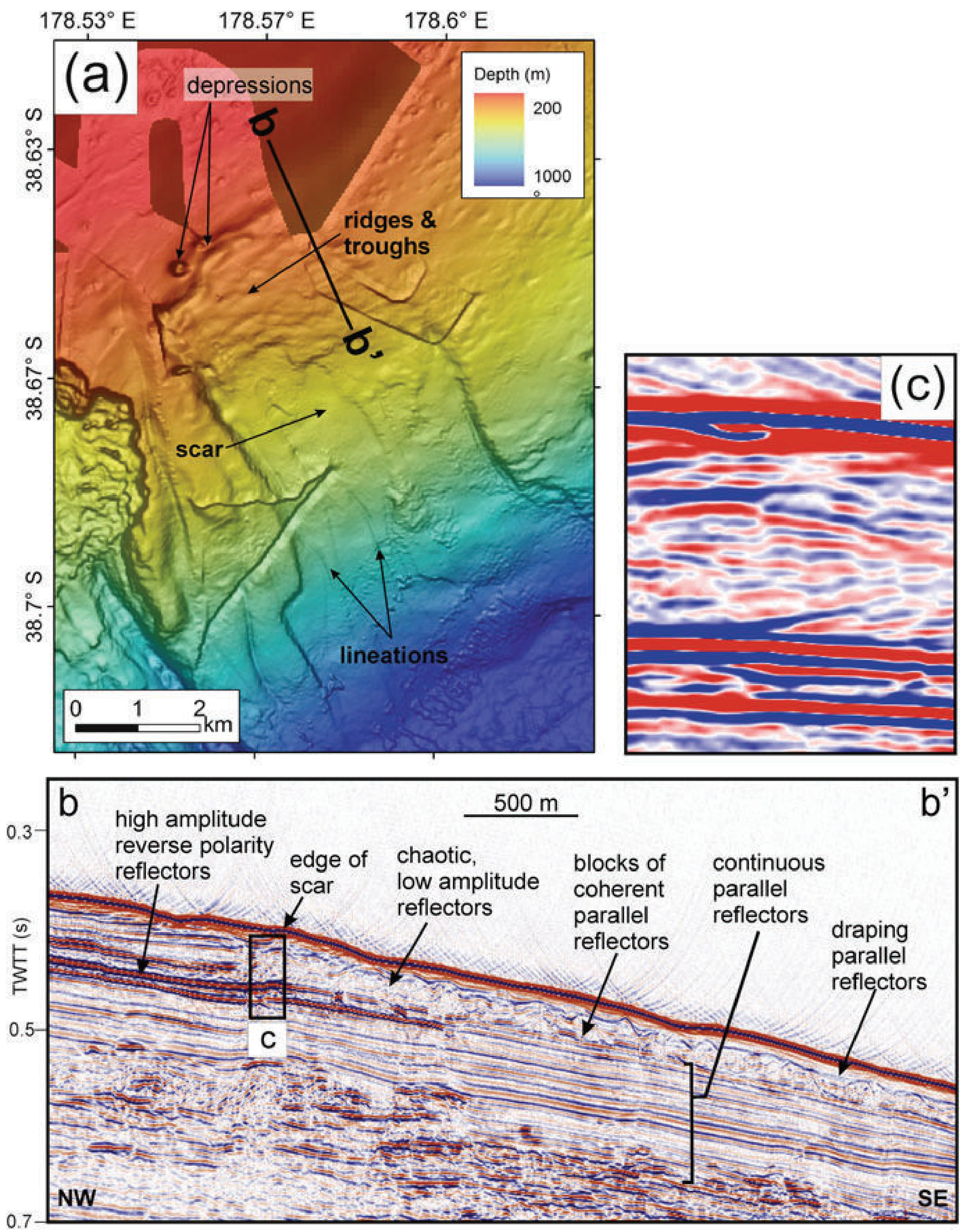

Fig. 42.2 (**a**) Bathymetric map of study area draped on a slope gradient map and showing principal morphologic elements of the scar. (**b**) Seismic reflection profile P3106 across the scar. (**c**) Enlarged section of profile P3106 showing reverse polarity of high amplitude reflector

reflectors, although triangular blocks of coherent, parallel, downslope-dipping reflectors are visible. This unit has a variable thickness, with a maximum of 40 m. The base of this chaotic unit is a planar reflector that connects with the high amplitude reflector further upslope. The chaotic unit is also covered by a draping unit of parallel reflectors, which is characterised by irregular thickness and reaches a maximum thickness of 35 m.

42.5 Discussion and Conclusions

42.5.1 *Nature of Mass Movement*

The downslope-dipping, parallel seismic reflectors across the study area are interpreted as layers in a stratified sediment package (Mountjoy et al. 2009). We infer that the material in this package is similar to that which failed in the adjacent Tuaheni Landslide Complex. This consisted of muddy sedimentary deposits, which accumulated during periods of eustatic sea level lowering, overlain by a Holocene hemipelagic succession (Carter and Manighetti 2006; Paquet et al. 2009). The ridge and trough morphology, and the chaotic seismic sequence with isolated blocks of coherent reflectors, are signature characteristics of submarine spreading (Micallef et al. 2007). We therefore interpret the upper section of the elongated scar documented across the study area as evidence of a submarine spreading event that comprised thin, extensional deformation of the lowstand units, occurring along stratigraphic surfaces, and which was later draped by Holocene sedimentation. This mode of failure corresponds to model 2 proposed by Micallef et al. (2007) for the Storegga Slide, where a thin slab ruptures under tension into a series of coherent blocks that translate and tilt downslope along a quasi-planar failure plane. The downslope section of the scar has undergone a higher degree of sediment evacuation, likely a result of translational sliding or more plastic deformation. The lineations may correspond to furrows eroded by debris flows into the failure surface.

42.5.2 *Role of Shallow Gas*

Limit equilibrium modelling by Micallef et al. (2007) showed how spreading can be pre-conditioned or triggered by three processes – loss of support, increase in total weight upslope, and an increase in pore pressure. Loss of support is a potential trigger of spreading in the region because of sediment evacuation in the downslope section of the scar. We exclude increase in total weight upslope as a potential cause because there are no indications of loading of sediment from a slope failure in the seismic data. An increase in pore pressure is also a likely cause of spreading in the study area. We interpret the high amplitude and reverse polarity reflectors in Fig. 42.2b as the top of an accumulation of gas within the sediments. The circular depressions, which we interpret as pockmarks, provide additional evidence of sub-seafloor overpressure. We are not able to determine whether the gas has biogenic or thermogenic origin. In bubble phase, gas is known to markedly increase the pore pressure, which decreases the effective stress of the seafloor sediment, creating weak layers that are prone to failure (Crutchley et al. 2010; Field 1990). In our study area this effect is enhanced by the low permeability of the fine-grained material that failed. The absence or low quantities of shallow gas in the elongated scar, and the correspondence of the depth of failure with that of the shallow gas, indicate that the latter has played a key role in establishing the failure surface. Additionally, dynamic changes in pore pressure may have been triggered by two factors. The first is a drop in sea level during the Last Glacial Maximum, with an associated reduction in effective stress as gas came out of solution due to lower hydrostatic pressures. This could explain why the absence of gas is more noticeable in the deeper part of the slope, where the reduction of the hydrostatic pressure would have been more pronounced. The second factor is seismic loading. The active fault most proximal to the study area is the Ariel Bank Fault (Fig. 42.1b), which is inferred to have a late Quaternary displacement rate in the range of 3.0–6.5 mm year^{-1} (Barnes et al. 2002). Peak ground acceleration, estimated from probabilistic seismic hazard modelling of regional earthquake sources, is in the order of 0.3–0.4 g with a return time of 475 years (Stirling et al. 2002). Some moderately large magnitude historic earthquakes have also occurred in the vicinity (e.g. the 1931 M7.8 Napier earthquake). The escarpment crossing the western boundary of the scar and the lineations may also be interpreted as the location of a recently-active fault.

To evaluate the potential failure mechanisms and perform stability analyses that take into account the role of gas charging and seismic loading, there is the need to acquire long sediment cores and carry out in situ geotechnical measurements from the study area.

Acknowledgments This research was supported by funding from Marie Curie Career Integration Grant PCIG13-GA-2013-618149 within the 7th European Community Framework Programme, New Zealand Ministry for Business Innovation and Employment, NIWA Core Funding under Coasts and Oceans Research Programme 1 (2013/14 SCI), DFG (Deutsche Forschungsgemeinschaft), and the Royal Society of New Zealand International Mobility Fund contract ISATB09-37. We are indebted to the TAN1404 shipboard party, and the captain, crew and technicians of *RV Tangaroa*. We thank Nicole Baeten and David Amblas for their insightful reviews.

References

Alexander CR, Walsh JP, Orpin AR (2010) Modern sediment dispersal and accumulation on the outer poverty continental margin. Mar Geol 270:213–226

Baeten NJ, Laberg JS, Forwick M et al (2013) Morphology and origin of smaller-scale mass movements on the continental slope off northern Norway. Geomorphology 187:122–134

Barnes PM, Nicol A, Harrison T (2002) Late Cenozoic evolution and earthquake potential of an active listric thrust complex above the Hikurangi subduction zone, New Zealand. Geol Soc Am Bull 114:1379–1405

Barnes PM, Lamarche G, Bialas J et al (2010) Tectonic and geological framework for gas hydrates and cold seeps on the Hikurangi subduction margin, New Zealand. Mar Geol 272:26–48

Beavan J, Tregoning P, Bevis M et al (2002) Motion and rigidity of the Pacific Plate and implications for plate boundary deformation. J Geophys Res 107:2261

Carter L, Manighetti B (2006) Glacial/interglacial control of terrigenous and biogenic fluxes in the deep ocean off a high input, collisional margin: a 139kyr-record from New Zealand. Mar Geol 226:307–322

Crutchley GJ, Geiger S, Pecher I et al (2010) The potential influence of shallow gas and gas hydrates on sea floor erosion of Rock Garden, an uplifted ridge offshore of New Zealand. Geo-Mar Lett 30:283–303

Dikau R, Brunsden D, Schrott L et al (1996) Landslide recognition: identification, movement and causes. Wiley, Chichester

Field ME (1990) Submarine landslides associated with shallow seafloor gas and gas hydrates off Northern California, In: AAPG (ed) Fifth circum-pacific energy and mineral resources conference, Honolulu

Field ME, Gardner JV, Jennings AE et al (1982) Earthquake-induced sediment failures on a 0.25° slope, Klamath River delta, California. Geology 10:542–546

Gauer P, Kvalstad TJ, Forsberg CF et al (2005) The last phase of the Storegga Slide: simulation of retrogressive slide dynamics and comparison with slide-scar morphology. Mar Petrol Geol 22:171–178

Kanibir A, Ulusay R, Aydan O (2006) Assessment of liquefaction and lateral spreading on the shore of Lake Sapanca during the Kocaeli (Turkey) earthquake. Eng Geol 83:307–331

Kukowski N, Greinert J, Henrys S (2010) Morphometric and critical taper analysis of the Rock Garden region, Hikurangi Margin, New Zealand: implications for slope stability and potential tsunami generatin. Mar Geol 272:141–153

Kvalstad TJ, Andersen L, Forsberg CF et al (2005) The Storegga slide: evaluation of triggering sources and slide mechanisms. Mar Pet Geol 22:245–256

Lastras G, Canals M, Urgeles R (2003) Lessons from sea-floor and subsea-floor imagery of the BIG'95 debris flow scar and deposit. In: Locat J, Mienert J (eds) Submarine mass movements and their consequences. Kluwer Academic Publishers, Dordrecht, pp 425–431

Lastras G, Canals M, Amblas D et al (2006) Eivissa slides, western Mediterranean sea: morphology and processes. Geo-Mar Lett 26:225–233

Micallef A, Masson DG, Berndt C et al (2007) Morphology and mechanics of submarine spreading: a case study from the Storegga Slide. J Geophys Res 112:F03023

Micallef A, Masson DG, Berndt C et al (2009) Development and mass movement processes of the north-eastern Storegga Slide. Quat Sci Rev 28:433–448

Micallef A, Georgiopoulou A, Le Bas T et al (2013) The Malta-Sicily escarpment: mass movement dynamics in a sediment-undersupplied margin. In: Krastel S et al (eds) Submarine mass movements and their consequences. Springer International Publishing, Switzerland, pp 317–328

Mountjoy JJ, Barnes PM (2011) Active upper-plate thrust faulting in regions of low plate-interface coupling, repeated slow slip events, and coastal uplift: example from the Hikurangi Margin, New Zealand. Geochem Geophys Geosyst 12:Q01005

Mountjoy JJ, McKean J, Barnes PM et al (2009) Terrestrial-style slow-moving earthflow kinematics in a submarine landslide complex. Mar Geol 267:114–127

Paquet F, Proust JN, Barnes PM et al (2009) Inner-forearc sequence architecture in response to climatic and tectonic forcing since 150 Ka: Hawke's Bay, New Zealand. J Sediment Res 79:97–124

Pedley KL, Barnes PM, Pettinga JR et al (2010) Seafloor structural geomorphic evolution of the accretionary frontal wedge in response to seamount subduction, poverty indentation, New Zealand. Mar Geol 270:119–138

Piper DJW, Cochonat P, Morrison ML (1999) The sequence of events around the epicentre of the 1929 Grand Banks earthquake: initiation of debris flows and turbidity currents inferred from sidescan sonar. Sedimentology 46:79–97

Rohn J, Resch M, Schneider H et al (2004) Large-scale lateral spreading and related mass movements in the Northern Calcareous Alps. Bull Eng Geol Environ 63:71–75

Stirling MW, McVerry GH, Berryman KR (2002) A new seismic hazard model for New Zealand. Bull Seismol Soc Am 92:1878–1903

Vanneste M, Mienert J, Bünz S (2006) The Hinlopen Slide: a giant, submarine slope failure on the northern Svalbard margin, Arctic Ocean. Earth Planet Sci Lett 245:373–388

Varnes DJ (1978) Slope movement types and processes. In: Schuster RL, Krisek RJ (eds) Landslides, analysis and control. National Academy of Sciences, Transportation Research Board, Special Report 176, pp 11–33